

## Comparison of EPRI Safety Valve Test Data With Analytically Determined Hydraulic Results

L.C. Smith, K.S. Howe

*Nuclear Technology Division, Westinghouse Electric Corporation, P.O. Box 355,  
Pittsburgh, Pennsylvania 15230, U.S.A.*

### SUMMARY

NUREG-0737 (November 1980) and all subsequent U.S. NRC generic follow-up letters require that all operating plant licensees and applicants verify the acceptability of plant specific pressurizer safety valve piping systems for valve operation transients by testing. To aid in this verification process, the Electric Power Research Institute (EPRI) conducted an extensive testing program at the Combustion Engineering Test Facility. Pertinent tests simulating dynamic opening of the safety valves for representative upstream environments were carried out. Different models and sizes of safety valves were tested at the simulated operating conditions. Transducers placed at key points in the system monitored a variety of thermal, hydraulic and structural parameters. From this data, a more complete description of the transient can be made.

The EPRI test configuration was analytically modeled using a one-dimensional thermal hydraulic computer program that uses the method of characteristics approach to generate key fluid parameters as a function of space and time. The conservative equations are solved by applying both the implicit and explicit characteristic methods. Unbalanced or wave forces were determined for each straight run of pipe bounded on each side by a turn or elbow. Blowdown forces were included, where appropriate. Several parameters were varied to determine the effects on the pressure, hydraulic forces and timings of events. By comparing these quantities with the experimentally obtained data, an approximate picture of the flow dynamics is arrived at. Two cases in particular are presented. These are the hot and cold loop seal discharge tests made with the Crosby 6M6 spring-loaded safety valve.

Included in the paper is a description of the hydraulic code, modeling techniques and assumptions, a comparison of the numerical results with experimental data and a qualitative description of the factors which govern pipe support loading.

## 1.0 INTRODUCTION

In November of 1980, the Nuclear Regulatory Commission (NRC) issued NUREG-0737. Under NUREG 0737, Section II.D.1, "Performance Testing of BWR and PWR Relief and Safety Valves", all operating plant licensees and applicants are required to conduct testing to qualify the reactor coolant system relief and safety valves under expected operating conditions for design-basis transients and accidents. In addition to the qualification of valves, the operability and structural integrity of the as-built pressurizer safety and relief valve (PSARV) discharge piping and supports must also be demonstrated on a plant specific basis.

In response to these requirements, a program for the performance testing of PWR safety and relief valves was formulated by EPRI. The primary objective of the Test Program was to provide full scale test data confirming the operability of the reactor coolant system power operated relief valves and safety valves for expected operating and accident conditions. The second objective of the program was to obtain sufficient piping thermal hydraulic load data to permit confirmation of models which may be utilized for plant unique analysis of PSARV discharge piping systems. The program was designed to envelope the various existing piping system configurations, the assortment of valves currently installed in various plants, and the different types of fluid inlet and discharge conditions which could exist.

Westinghouse has been and is heavily involved in applying the results of the EPRI test program. As is typical with most test results, it was decided that the application of the EPRI test results could best be carried out in two stages. First, the thermal hydraulic analyses and dynamic structural analysis computer programs are benchmarked against the test results. In the second stage the benchmarked computer codes are used to carry out computer analysis of various piping configurations subjected to various fluid loading conditions. The results of these analyses are then used to evaluate the acceptability of these various piping systems.

Upstream piping lengths, valve flow rates, axial and lateral supports in addition to applied forcing functions all effect and all determine the PSARV piping and support design. The thermal hydraulic forces resulting from valve discharge are often the most important design consideration.

The comparative material presented in this paper considers thermal hydraulic and piping data from EPRI tests No. 917 and No. 908, the hot and cold loop seal tests, respectively, with the Crosby 6M6 spring-loaded safety valve mounted on the test configuration. These two specific tests were chosen since they are representative of the majority of PSARV systems on Westinghouse supplied Pressurized Water Reactors. Figure 1 illustrates the test configuration under discussion including the location of pertinent instrumentation.

## 2.0 THERMAL HYDRAULIC ANALYSIS

### 2.1 GENERAL

A Westinghouse proprietary computer code was used to perform the transient hydraulic analysis for the system. This program uses the Method of Characteristics<sup>[1,2]</sup> approach to generate fluid parameters as a function of time. One-dimensional fluid flow calculations applying both the implicit and explicit characteristic methods were performed.

The determination of the force requires that key variables be first determined for all segments of the piping for the duration of the transient. For the transient under consideration, a thermal-hydraulic analysis was performed to determine the values of these variables as a function of space and time for all piping segments. The basic one-dimensional equations of mass, energy and momentum conservation which must be solved to determine  $\rho$  and  $V$  are:

$$\text{CONTINUITY: } \frac{\partial \rho}{\partial t} + \frac{\partial(\rho V)}{\partial Z} = 0 \quad (1)$$

$$\text{MOMENTUM: } \frac{\partial}{\partial t} (\rho V) + \frac{\partial(\rho V^2)}{\partial Z} + \frac{\partial P}{\partial Z} = F + \rho g \cos \theta \quad (2)$$

$$\text{ENERGY: } \frac{\partial h}{\partial t} + V \frac{\partial h}{\partial Z} - \frac{1}{J\rho} \left( \frac{\partial P}{\partial t} + V \frac{\partial P}{\partial Z} \right) = \frac{q'''}{\rho} \quad (3)$$

These continuity and momentum equations can be transformed to the following characteristic equations:

$$\frac{dz}{dt} = V + c \quad (\text{left characteristic}) \quad (4)$$

$$\frac{dP}{dt} + \rho c \frac{dV}{dt} = c(F + \rho g \cos \theta) - \frac{q'''}{\rho} \frac{c^2}{\frac{\partial h}{\partial \rho}} \quad (5)$$

$$\frac{dz}{dt} = V - c \quad (\text{right characteristic}) \quad (6)$$

$$\frac{dP}{dt} - \rho c \frac{dV}{dt} = -c(F + \rho g \cos \theta) - \frac{q'''}{\rho} \frac{c^2}{\frac{\partial h}{\partial \rho}} \quad (7)$$

where the sonic velocity is defined as

$$c^2 = \frac{-\partial h / \partial \rho}{\frac{\partial h}{\partial \rho} - \frac{1}{\rho J}} \quad (8)$$

In a similar fashion, the energy equation may be transformed into the following characteristic equation along the line  $\frac{dz}{dt} = V$ .

$$\rho \frac{dh}{dt} - \frac{1}{J} \frac{dP}{dt} = q''' \quad (9)$$

and  $z$  = variable of length       $P$  = pressure       $\theta$  = angle off vertical  
 $t$  = time       $\rho$  = fluid density       $J$  = conversion factor  
 $V$  = fluid velocity       $F$  = flow resistance       $h$  = enthalpy  
 $c$  = sonic velocity       $g$  = gravity       $q'''$  = heat generation rate

The appropriate equations can be expressed as finite difference equations, either explicitly or implicitly. At each time step, the left characteristic equation, Eq. (5), and the right characteristic equation, Eq. (7), are solved simultaneously using the band elimination method. The enthalpies are calculated either through the mass balance, Eq. (1), and the energy balance, Eq. (3), or through the third characteristic equation, Eq. (9).

The force time histories acting on a nuclear power plant piping configuration can be determined by applying the integral form of the momentum equation<sup>[3]</sup> given by

$$\iint P dA + \iiint B dv = \iint V(\rho V dA) + \frac{\partial}{\partial t} \iiint \rho V dv \quad (10)$$

For a bounded segment, which is a section of pipe bounded at either end by an elbow or bend, the acting force is the wave force associated with the unsteady flow. This force is represented by the last term of Eq. (10).

Fluid acceleration<sup>[4,5]</sup> inside the pipe generates reaction forces on all bounded segments. These forces can be expressed in terms of the fluid properties available from the transient hydraulic analysis. The wave force can be expressed in vector form as:

$$\vec{F} = \frac{1}{g_c} \frac{\partial}{\partial t} \int_V \rho \vec{V} dv \quad (11)$$

From this equation, the total force on the pipe can be derived:

$$F_{\text{pipe}} = \frac{r_1 (1 - \cos \alpha_1)}{g_c \sin \alpha_1} \frac{\partial W}{\partial t} \Big|_{\text{Bend 1}} + \frac{r_2 (1 - \cos \alpha_2)}{g_c \sin \alpha_2} \frac{\partial W}{\partial t} \Big|_{\text{Bend 2}} + \frac{1}{g_c} \int_{\text{pipe}} \frac{\partial W}{\partial t} dl \quad (12)$$

A = piping flow area      α = angle of elbow      r = elbow radius of  
v = volume                      W = mass acceleration                      curvature  
F = force                      B = body force                      g<sub>c</sub> = gravitational constant

All other terms are previously defined.

F<sub>pipe</sub> defines the wave force acting on the bounded pipe. For an unbounded pipe or open segment, the total force is the sum of the wave force along the pipe length and the blowdown force at the pipe end. This blowdown force is defined as the sum of the pressure force and momentum force and is given by the first and third term respectively of Eq. (10). The total force on any open segment is then given by:

$$F_{\text{open segment}} = (F_{\text{pipe}}) + (P + \rho V^2) \frac{A}{g_c} \quad (13)$$

Equation 12

where P, ρ and V are taken at the pipe end.

Blowdown forces were included in the total analytically determined force where applicable. (i.e. sensor ME34/35)

## 2.2 TEST 908 AND TEST 917 DESCRIPTION<sup>[6]</sup>

Test 908 was conducted to represent a cold water loop seal discharge followed by steam through a 6M6 spring-loaded pressurizer safety valve built by the Crosby Valve and Gage Company. The water temperature in the loop seal near the valve inlet was initially 100°F. Figure 2 represents the temperature profile for test 908. The valve began to open when the pressure in the accumulator reached approximately 2560 psia. The valve stem oscillated at high frequencies during the early part of the discharge transient for roughly 900 milliseconds. The valve reached full open position 15 milliseconds later. The pressure in the accumulator tank upstream of the valve at the time the valve was fully open was approximately 2690 psia.

Test 917 was similar to Test 908 except the water seal temperature was significantly hotter. The valve inlet loop seal temperature was about 300°F. Figure 3 illustrates the test 917 temperature profile. The valve began to open when the accumulator pressure reached 2460 psia. As in test 908, the valve stem oscillated at about 200 Hz for roughly 650 milliseconds. The valve reached full open position 90 milliseconds later. The accumulator tank pressure was 2650 psia at the time the valve was fully open.

### 2.3 THERMAL HYDRAULIC MODELING

The thermal hydraulic system model was very similar for both tests evaluated. Major differences were only in the initial fluid conditions of the system.

For both tests analytically modeled and evaluated, the safety valve was assumed to linearly go from the fully closed to the fully open position in 40 milliseconds. The safety valve full-open flow area of  $0.022 \text{ ft}^2$  was used in the model. This area is slightly smaller than the Crosby M-orifice area of  $0.025 \text{ ft}^2$  for the tested valve. Flow visualization experiments performed by Sallet<sup>[7]</sup> show that the orifice area of a valve may not be the actual area of flow. Because of sharp edges, significant flow separation occurs in the valve internals resulting in a reduced flow area. Using this reduced area gives a good analytical to test match of the full open valve flow rate ( $\sim 463,000 \text{ lb/hr}$  versus  $\sim 460,000 \text{ lb/hr}$ ).

The upstream pressure boundary at the accumulator tank was presumed to be steam conditions at 2700 psia. Appropriate water seal temperatures were used. Saturated conditions consistent with a pressure slightly above atmospheric pressure were input as initial conditions in the downstream piping. All pertinent data, including friction factors, loss factors and flow areas, were based upon representative calculations and the system layout.

For test 908, the water seal initially has an obvious interface with the steam upstream of it. This interface was included in the model and was retained until it passed through the valve, at which time it was dispersed (removed). Following dispersion, the tail of the loop seal can mix with the steam that drives it. The other end of the seal started out in contact with the valve. An interface was placed here to allow the density of the loop seal to remain at a high value. Once the loop seal entered the final very long horizontal run in the facility, it is believed that some combination of pipe wall friction and separation from rounding the elbow caused the flow to form a mixed, probably nonhomogeneous flow. It is therefore not representative to retain the leading interface beyond this elbow.

For test 917, the interface between the water seal and the upstream steam was included in the model and was retained, as in the test 908 model, until the interface passed through the valve. At this point, it was allowed to disperse. The other end of the seal started out at the valve. To model the flashing/mixing affect, the leading interface was allowed to disperse just downstream of the safety valve.

Figure 4 illustrates the location of pertinent force time histories resulting from the thermal hydraulic evaluation.

### 2.4 SPECIFIC THERMAL HYDRAULIC RESULTS

EPRI Tests 908 and 917 conducted at the Combustion Engineering Test Facility showed that forces are reduced significantly with increased safety valve-seal temperatures. Analytical results substantiate this. For example, Test 908, the cold loop seal test, showed a peak force of approximately 180 kips at sensor WE32/WE33 (see Figure 1 for location). Test 917, the hot loop seal test, registered approximately 13 kips at the same sensor. Based upon engineering judgement, significant flashing of hot water near the valve occurred for Test 917, thus reducing the downstream loads accordingly.

Figures 5, 6 and 7 illustrate a comparison of the thermal hydraulically calculated results versus experimental results for Test 908, the cold water discharge followed by

steam case. Figure 5 shows the pressure time histories for PT9, which is located just downstream of the valve. Figures 6 and 7 illustrate, respectively, the force time histories of the horizontal run (WE28/WE29) and the long vertical run (WE32/WE33) immediately downstream of the safety valve. Significant structural damping in the third segment after the valve was noticed at the test and was verified by structural analyses. Consequently, a comparison of force WE30/WE31 was not presented here. No usable test data for sensor WE34/WE35 was available for Test 908.

Figures 8 through 12 illustrate a comparison of calculated versus experimental results for Test 917, the hot water discharge followed by steam case. Figure 8 shows the pressure time histories for PT9. Figures 9, 10, 11 and 12 illustrate, respectively, the thermal hydraulically calculated and the experimentally determined force time histories for (WE28/WE29), (WE32/WE33), (WE30/WE31) and (WE34/ WE35). Blowdown forces were included in the total analytically calculated force for WE34/WE35 as this section of piping vents to the atmosphere.

Figures 5 through 12 illustrate a very good analytical to experimental comparison.

### 3.0 CONCLUSIONS AND RECOMMENDATIONS

The pressurizer safety valves and associated piping, located on top of the pressurizer, provide overpressure protection for the Reactor Coolant System of a Pressurized Water Reactor. On most of the Westinghouse Nuclear Steam Supply Systems a water seal is established directly upstream of the safety valves to help reduce the potential for valve leakage. Experience has shown that elimination of this seal significantly increases the probability of valve leakage and correspondingly decreases the up-time or reliability of the Pressurized Water Reactor. EPRI test data has shown that cold loop seals could result in excessively high downstream piping and support loadings. The same tests have illustrated that hot loop seals would result in significantly reduced piping and support loads subsequent to discharge of the safety valves. Therefore, a system that includes reasonably hot loop seals immediately upstream of the safety valves would result in an optimum design for the overpressure protection system located atop the pressurizer of a Pressurized Water Reactor because it would minimize piping and support loadings subsequent to discharge through the valves and because it would minimize the potential for valve leakage during normal plant operation.

### 4.0 ACKNOWLEDGEMENTS

We wish to acknowledge Dr. K. C. Chang and Mr. A. C. Spencer for their leadership and motivation.

### 5.0 REFERENCES

- /1/ Nakamura, S., M.A. Berger and A.C. Spencer, "One-Dimensional Implicit Characteristic Method for Compressible Two Phase Coolant Flow," Proceedings of the Conference on Computational Methods in Nuclear Engineering, CONF-750413, 1975.
- /2/ Nakamura, S. and A. C. Spencer, "Implicit Characteristic Method for One-Dimensional Fluid Flow," Trans. Amer. Nucl. Soc. 17, pp. 247-249, (1973).
- /3/ Hsu, M., J. Weisman and J. W. Redmond, "An Evaluation of Time-Dependent Loading Analysis on a Piping Network Using RELAP4/REPIPE," Nucl. Technol. 53, pp 58-63 (1981).

- /4/ Moody, F. J., "Fluid Reaction and Impingement Loads," Volume I, ASCE Specialty Conf. on Structural Design of Nuclear Plant Facilities, Chicago, IL, December 17-18, 1973, American Society of Civil Engineers, New York, 1976.
- /5/ Moody, F. J., "Time-Dependent Pipe Forces Caused by Blowdown and Flow Stoppage," ASME Paper 73-FE-23.
- /6/ Application of RELAP5/MOD1 for Calculation of Safety and Relief Valve Discharge Piping Hydrodynamic Loads, EPRI-NP-2479-LD, July, 1982.
- /7/ Sallet, D. W., "Thermal Hydraulics of Valves for Nuclear Applications," The Second International Topical Meeting on Nuclear Reactor Thermal-Hydraulics, January, 1983, pp. 111-134.

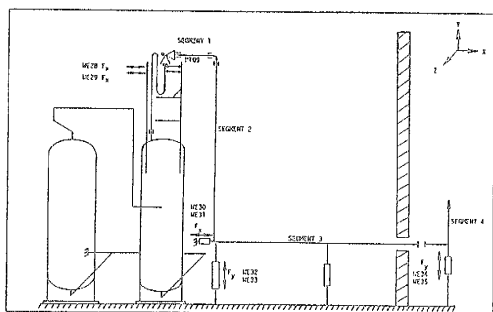


FIGURE 1: PERTURBATION MEASUREMENT LOCATIONS - EPRI TEST

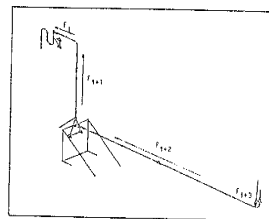


FIGURE 4: LOCATION OF PERTURBATION FORCE TIME-HISTORIES FROM THE THERMAL-HYDRAULIC ANALYSIS

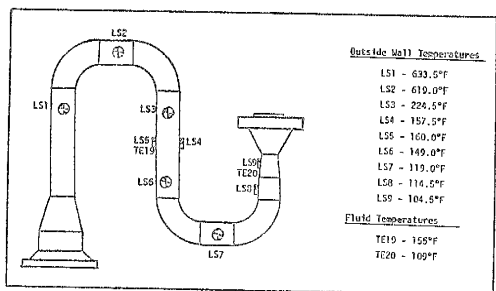


FIGURE 2: LOOP SEAL TEMPERATURE PROFILE FOR TEST 908

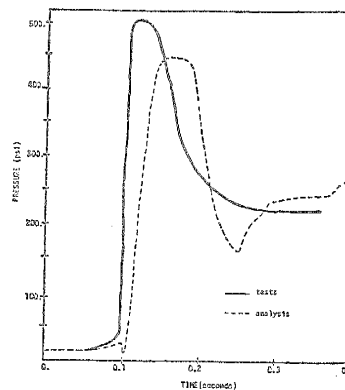


FIGURE 5: COMPARISON OF THE EPRI PRESSURE TIME-HISTORY FOR PIPES FROM TEST 908 WITH THE ANALYTICALLY CALCULATED PRESSURE TIME-HISTORY

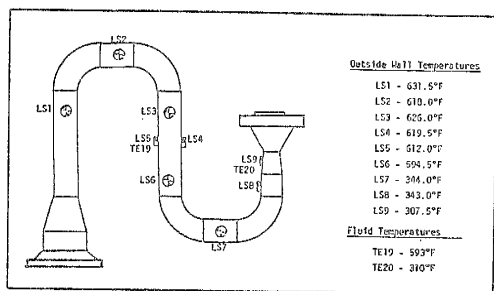


FIGURE 3: LOOP SEAL TEMPERATURE PROFILE FOR TEST 917

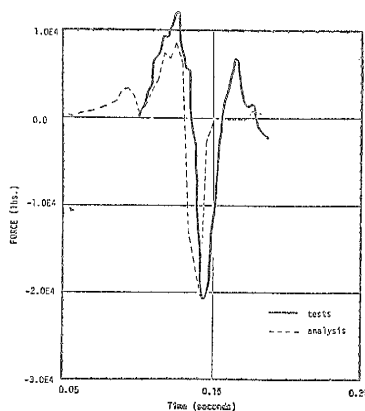


FIGURE 6: COMPARISON OF THE EPRI FORCE TIME-HISTORY FOR WETS AND W22 FROM TEST 908 WITH THE ANALYTICALLY CALCULATED FORCE TIME-HISTORY

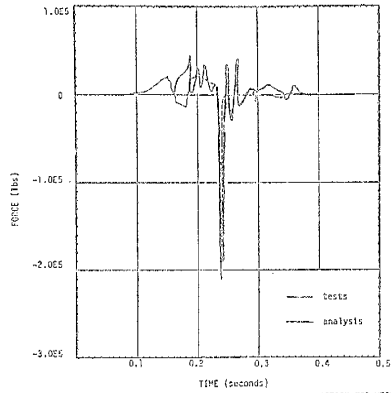


FIGURE 7: COMPARISON OF THE EPRI FORCE TIME-HISTORY FOR WE32 AND WE33 FROM TEST 903 WITH THE ANALYTICALLY CALCULATED FORCE TIME-HISTORY

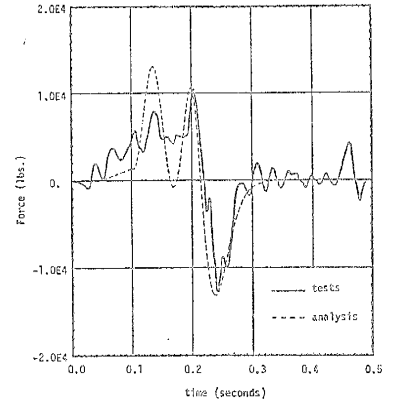


FIGURE 10: COMPARISON OF THE EPRI FORCE TIME-HISTORY FOR WE32 AND WE33 FROM TEST 917 WITH THE ANALYTICALLY CALCULATED FORCE TIME-HISTORY

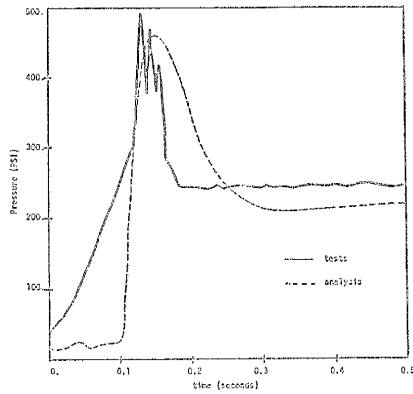


FIGURE 8: COMPARISON OF THE EPRI PRESSURE TIME-HISTORY FROM PT09 FROM TEST 919 WITH THE ANALYTICALLY CALCULATED PRESSURE TIME-HISTORY

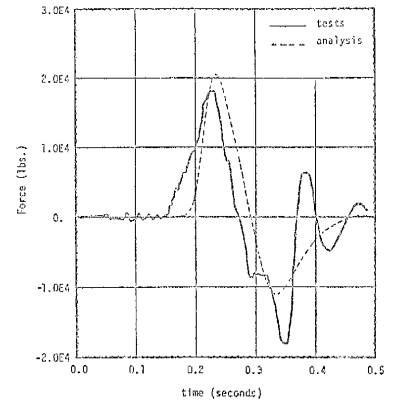


FIGURE 11: COMPARISON OF THE EPRI FORCE TIME-HISTORY FOR WE30 AND WE31 FROM TEST 917 WITH THE ANALYTICALLY CALCULATED FORCE TIME-HISTORY

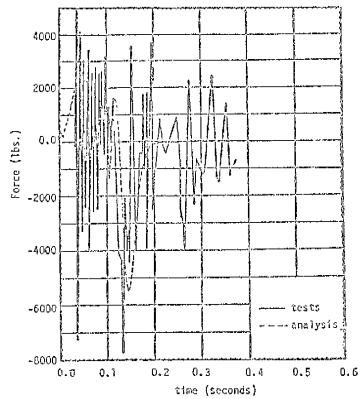


FIGURE 9: COMPARISON OF THE EPRI FORCE TIME-HISTORY FOR WE28 AND WE29 FROM TEST 917 WITH THE ANALYTICALLY CALCULATED FORCE TIME-HISTORY

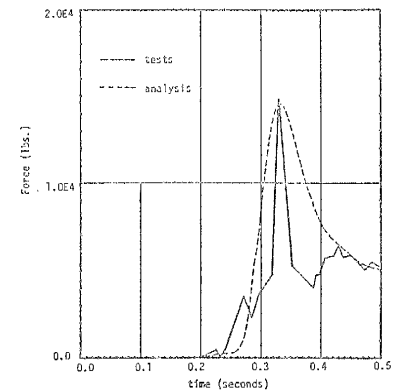


FIGURE 12: COMPARISON OF THE EPRI FORCE TIME-HISTORY FOR WE34 AND WE35 FROM TEST 917 WITH THE ANALYTICALLY CALCULATED FORCE TIME-HISTORY